2017 International Nuclear Atlantic Conference - INAC 2017
Belo Horizonte, MG, Brazil, October 22-27, 2017
ASSOCIAÇÃO BRASILEIRA DE ENERGIA NUCLEAR – ABEN

RECONSTRUCTED IMAGE QUALITY ANALYSIS OF AN INDUSTRIAL INSTANT NON-SCANNING TOMOGRAPHY SYSTEM WITH DIFFERENT TYPES OF COLLIMATORS BY THE MONTE CARLO SIMULATION.

Alexandre F. Velo[1], Diego V. Carvalho[1], Alexandre G. Alvarez[1], Margarida M. Hamada[1] and Carlos H. Mesquita[1]

[1] Instituto de Pesquisas Energéticas e Nucleares (IPEN / CNEN - SP)
Av. Professor Lineu Prestes 2242
05508-000 São Paulo, SP
afvelo@usp.br

ABSTRACT

The greatest impact of the tomography technology application currently occurs in medicine. The great success of medical tomography is due to the human body presents reasonably standardized dimensions with well-established chemical composition. Generally, these favorable conditions are not found in large industrial objects. In the industry there is much interest in using the information of the tomograph in order to know the interior of: (i) manufactured industrial objects or (ii) machines and their means of production. In these cases, the purpose of the tomograph is to: (a) control the quality of the final product and (b) optimize production, contributing to the pilot phase of the projects and analyzing the quality of the means of production. In different industrial processes, e. g. in chemical reactors and distillation columns, the phenomena related to multiphase processes are usually fast, requiring high temporal resolution of the computed tomography (CT) data acquisition. In this context, Instant non-scanning tomograph and fifth generation tomograph meets these requirements. An instant non-scanning tomography system is being developed at the IPEN/CNEN. In this work, in order to optimize the system, this tomograph comprised different collimators was simulated, with Monte Carlo method using the MCNP4C. The image quality was evaluated with Matlab® 2013b, by analysis of the following parameters: contrast to noise (CNR), root mean square ratio (RMSE), signal to noise ratio (SNR) and the spatial resolution by the Modulation Transfer Function (MTF(f)), to analyze which collimator fits better to the instant non-scanning tomography. It was simulated three situations; (i) with no collimator; (ii) ?25 mm x 50 mm cylindrical collimator with a septum of ø5.0 mm x 50 mm; (iii) ø25mm x 50 mm cylindrical collimator with a slit septum of 24 mm x 5.0 mm x 50 mm.

1. INTRODUCTION

The industrial distillation system involves fast dynamic processes containing solid, liquid and gas mixtures. The distillation columns are usually built with steel and have large diameters and thicknesses that make their analysis unfeasible with conventional X-ray beams [1,2,3]. For this reason, gamma radioactive sources in the energy ranges of 317 keV (^{192}Ir), 662 keV (^{137}Cs) to 1250/1332.501 keV (^{60}Co) are preferable, instead of low X-ray energy sources [3].

In addition, the system should be adapted for different sizes of objects that are usually sited in a hostile environment, containing flammable superheated materials, occasionally subjected to high internal pressure and presenting many difficulties for placing CT devices around these objects. Besides, the phenomena related to multiphase processes are usually fast, requiring high time resolution of the CT data acquisition [1-4]. In such case, ideally, the tomography

system should be fixed and not need to move their sources and detectors around the object. Instant Non-Scanning and fifth generation topographies meet these requirements [5,6]. Additionally, the system should be light enough to be portable and easily installed.

In order to be applicable in the practical of industrial plants, an instant non-scanning tomography system is being developed. This industrial tomography is comprised by 5 sets of fourteen 1x2 inches (diameter and length) NaI(Tl) detectors and five shielding cases for radioactive sources. Each shielding case is placed diametrically opposite to a fan detector set as showed in Fig. 1 [3].

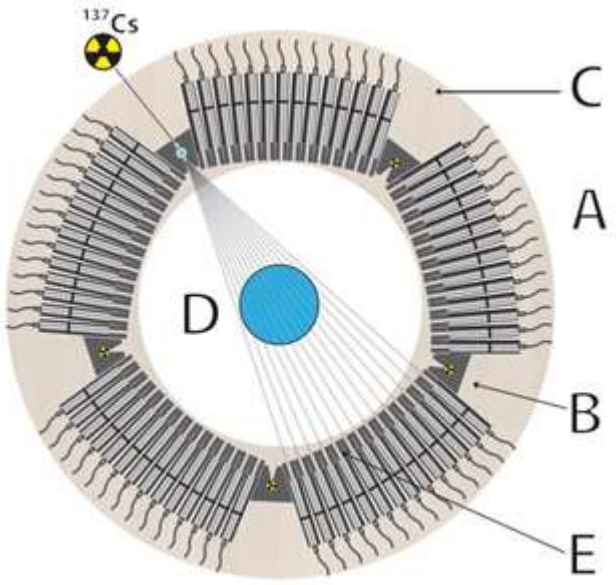

Figure 1: Instant Non-Scanning tomography design for multiphase analysis. NaI(Tl) detectors (A), radioactive shielding case (B), wooden platform (C), the multiphase object to be analyzed (D) and detector collimator (E) [3].

The NaI(Tl) detectors are capable to detect large range of energies, i.e. from 59.5412 keV 2^{41}Am to 1250/1332.501 keV ^{60}Co [7], then the choose of the source to be used depends on the material densities, wall thickness and dimension of the object to be evaluated by tomography measurements. Also, the proposed tomography system can be adjusted to the column or pipes by changing the number of detector set. Thus, the tomography system has the capacity of being adapted and applied for different objects types, such as, column or pipe sizes found usually in the industrial plants. The tomography system can be mounted on a wooden platform, which is lightweight to be replaced in future applications according to the challenges of new geometry, dimension of the objects and application requirements.

The MCNP code is a general purpose Monte Carlo radiation transport and designed to track different types of particles (neutrons, electrons, gamma rays, etc.) over a broad range of energies. The code obtains the solution of the problem by simulating individual particle trajectories and recording some aspects of their average behavior [3,8]. The process consists of following each of many particles since its emission from a source until it reaches an energy threshold; the particle energy is transferred to the matter by absorption, escape, physical cut-

off, and others. Probability distributions are randomly sampled using transport data to determine the outcome at each step of its trajectory. The quantities of interest are tallied along with estimates of the statistical precision of the results. The MCNP code can be used to simulate gamma-rays interactions which comprise: i) incoherent and coherent scattering; ii) the possibility of fluorescent emission after photoelectric absorption; iii) pair production with local emission of annihilation radiation and Bremsstrahlung effect [3, 9].

This work used the Monte Carlo N-Particle (MCNP) developed by Los Alamos National Laboratory [10] to simulate the Instant Non-Scanning Tomography system, with different types of collimators and evaluate the quality of the images in order to kwon which collimator meets the specificity of the tomography system in development.

2. MATERIAL AND METHODS

2.1. Monte Carlo Simulation

The simulation was carried with five sets of NaI(Tl) detectors (1 x 2 inches) and five 662 keV ^{137}Cs sources enclosed in a tungsten shielding cases. For this first purpose, each set is constituted of fourteen NaI(Tl) detectors, that is positioned diametrically opposite to a source shielding case as shown by Fig. 1. All five detector sets and the five radioactive source shielding cases are mounted on a wooden platform as shown in Fig. 1.

Three situations was performed; (i) with no collimator; (ii) 27 mm x 50 mm collimator with a septum of ø5.0 mm x 50 mm and (iii) 27mm x 50 mm collimator with a slit septum of 24 mm x 5.0 mm x 50 mm. The schemes of the collimators are presented by Fig 2.

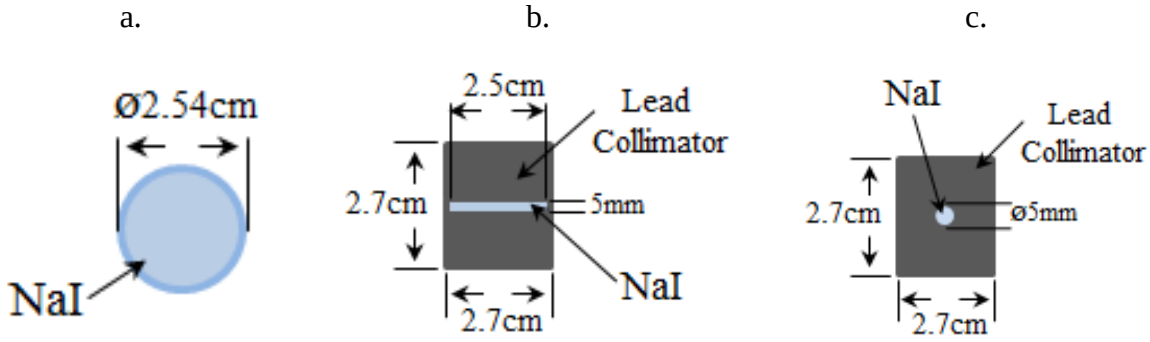

Figure 2: Proposed simulation, (a) no collimator; (b) slit collimator and (c) hole collimator

When performing the mathematical simulation of NaI(Tl) detectors, in order to obtain their response curves, some corrections should be made to improve the simulation approaching to the real case. Two of the main corrections are essential: the determination of the photon detection efficiency and the energy resolution, which is related to distinguish different peaks very close to each other in the energy spectrum [8, 11].

In practice, the energy resolution of the detector is given by the full width at half maximum (FWHM) of the Gaussian peak (pulses per channel) for a given energy [8, 12].
Some of the effects related to the photopeak are inherent to the electronic circuit of the spectrometric system which is not simulated by the MCNP. Thus, to optimize the detector response and consider these physical effects in the simulation, it is necessary to obtain experimentally adjustment parameters of the detector energy resolution and apply a MCNP code function to fits the Gaussian to the spectrum obtaining the proper corrections [8].

The MCNP fitting technique to take into account the resolution of the real detector, measured experimentally, consists of using a "FT8 GEB" card into the input file of the code. The tallied energy is broadened by sampling from Gaussian [3, 8].

A non-linear function adjusted by least-squares procedure was used as a input to the MCNP code, using a fitting function [9]. These parameters should be used with the Gaussian Energy Broadening (GEB) command in order to consider the energy resolution of the detector in the simulation [16]. GEB is a special treatment for tallies to better simulate a physical radiation detector in which energy peaks exhibit Gaussian energy broadening. These parameters were calculated in previous works [3, 8].

The detector simulation was based on the dimensions of the real NaI(Tl) detector used in the Instant non-scanning tomography.

For the estimation of the pulse height, a F8 tally was applied on MCNP code to obtain the deposited energy distribution per incident photon on the NaI(Tl) detector, where for each individual history, the tally accumulates the deposited energy. In order to obtain a good statistic counts, the histories number used was 11E+09.

2.2. Physical Measurements

A phantom was simulated to evaluate the physical parameters of the Instant Non-canning tomography system [3]. The phantom was composed of a cylindrical polymethylmethacrylate (PMMA (($\rho \approx 1.19$ g/cm3)) of Ø24cm x 20cm dimensions and an aluminum cylindrical bar ($\rho \approx 2.698$ g/cm3) of Ø7.5cm x 20cm inside the PMMA. The figure is illustrated by Fig. 3.

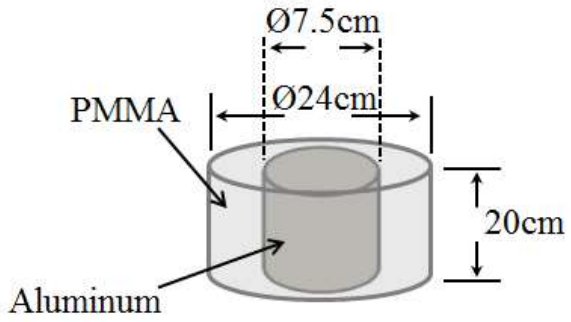

Figure 3: Simulated phantom for the physical analysis

The Root Mean Square Error (RMSE) was measured to evaluate which algorithm of reconstruction approaches the pixel values that correspond to the linear attenuation

coefficient, obtained by the reconstruction, to the theoretical values. This method is widely used to measure the quality of the image. The RMSE was calculated by the equation (1) [3].

$$RMSE = \sqrt{\frac{\sum_{i=1}^{N}(\mu_i - \widehat{\mu_i})^2}{N}} \tag{1}$$

where μ_i is the experimental pixel value obtained, $\widehat{\mu_i}$ is the theoretical linear attenuation coefficient. The theoretical image is presented by the Fig. 4.

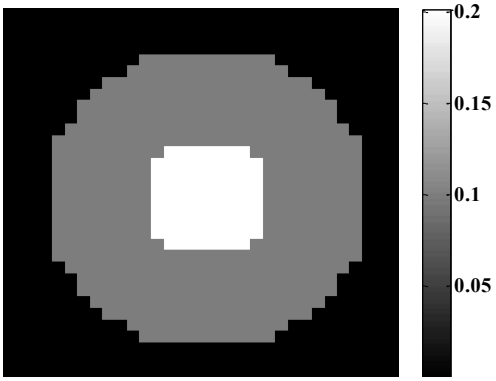

Figure 4: Theoretical image.

The Contrast to Noise Ratio (CNR) was measured placing regions of interest (ROIs) in the images obtained by the phantom (Fig. 2) with the different algorithms. A circular ROI was placed over the cylinder corresponding the aluminum (ROI A) and another ROI, with the same size of the ROI A, placed over the background, corresponding the PMMA (ROI B), then the values of the CNR was obtained by the equation (2) [13, 14].

$$CNR = \frac{|\overline{\mu_A} - \overline{\mu_B}|}{\sqrt{\frac{\sigma_A^2 + \sigma_B^2}{2}}} \tag{2}$$

where $\overline{\mu_A}$ is the mean pixel value of the ROI A, $\overline{\mu_B}$ is the mean pixel value of the ROI B, $\sigma_A$is the standard deviation of ROI A and σ_B is the standard deviation of the ROI B. The ROIs is represented on Fig. 5, where the red circle represents the ROI A and the blue circle represents the ROI B.

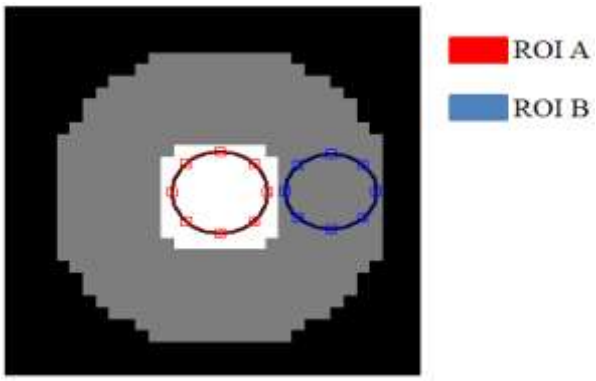

Figure 5: ROIs used to measure the CNR

The algorithm used to reconstruct the images was the Maximum Likelihood Expectation Maximization (MLEM) [15], in a matrix of 32x32. All physical measurements and reconstructions were performed by the Matlab 2013b®.

The most comprehensive metric used to measure and report spatial resolution of imaging systems is the modulation transfer function (MTF) [14, 16, 17]. Conventionally, the spatial resolution is estimated as the inverse of the value at 10% of MTF curve [14, 16, 17]. In the present work, MTF was calculated using the Edge Spread Function, commonly known as ESF parameter [16, 17].

3. RESULTS AND DISCUSSION

The ^{137}Cs spectrum obtained by the simulated NaI(Tl) detectors with no collimator, slit collimator and hole collimator are shown by Fig. 6.

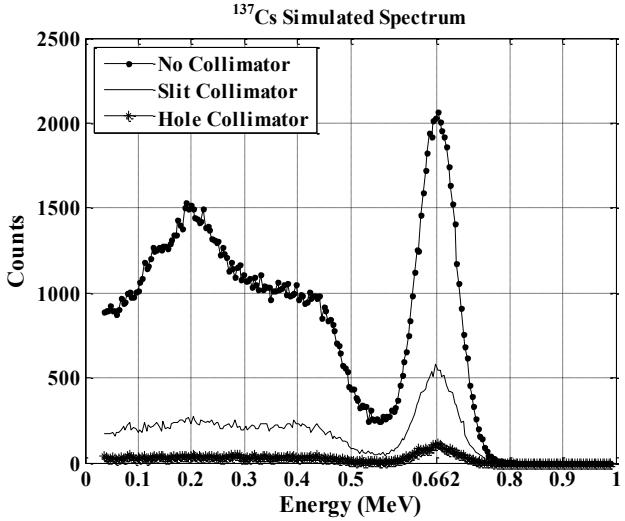

Figure 6: Simulated ^{137}Cs spectrum for no collimator, slit collimator and hole collimator

By Fig. 6 it is possible to observe that for the simulation with no collimator the sensitivity is higher than with collimators, and the ^{137}Cs spectrum obtained by the simulation with slit

collimator has higher sensitivity then the spectrum obtained by the hole collimator. The reconstructed images of the phantom (Fig. 3) obtained by the simulation of the Instant Non-Scanning tomography with different collimators are presented by the Fig. 7, where Fig. 7a. is the simulation with no collimator; Fig. 7b. is the simulation with slit collimator and Fig. 7c. is simulation with hole collimator.

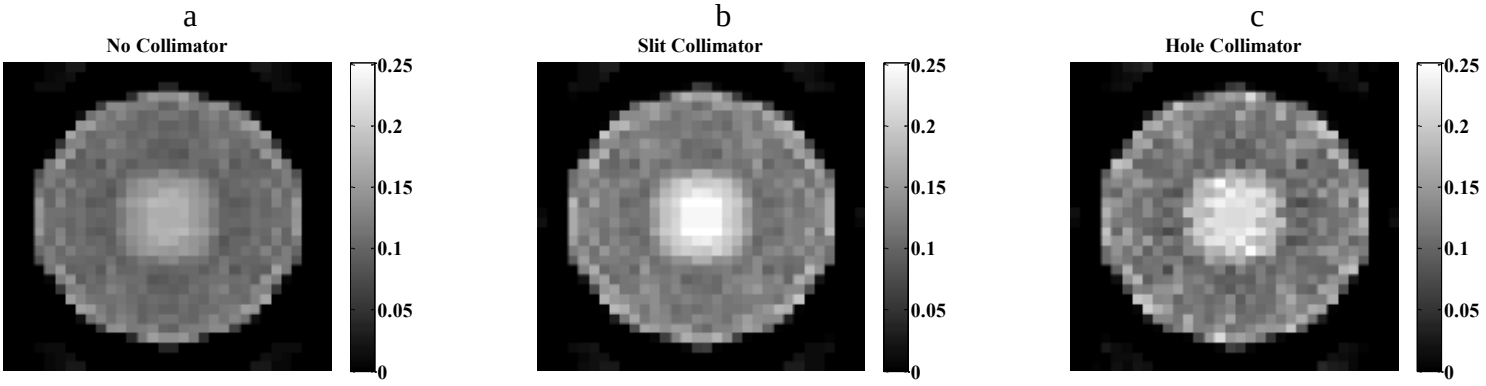

Figure 7. Reconstructed images of the simulated instant non-scannig with, (a) no collimator; (b) slit collimator and (c) hole collimator.

The RMSE parameter applied to perform the quality of the image for the three different simulations was calculated using equation (1), comparing the experimental images with the theoretical image. Fig. 8 shows the curve behavior for each simulation.

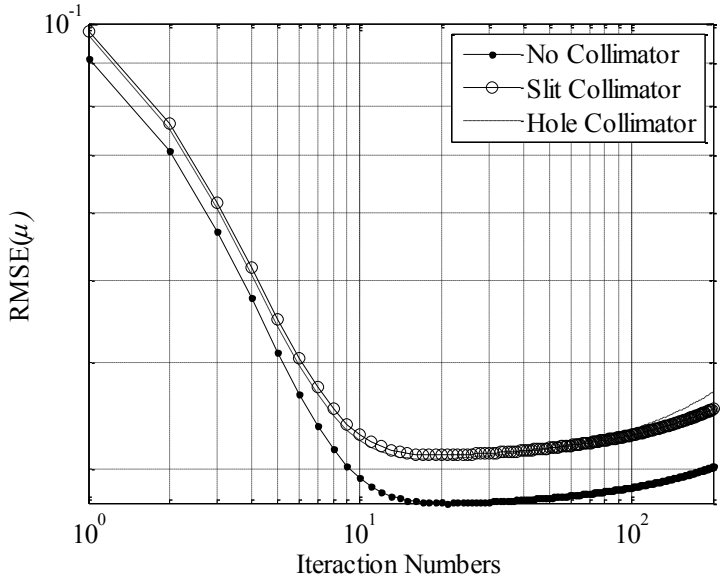

Figure 8: RMSE analysis for (a) no collimator; (b) slit collimator and (c) hole collimator.

Fig 8 shows that the simulation with no collimator approaches to the theoretical value more than the simulation with collimators, and the data obtained by the simulation with collimators did not presented any differences on the RMSE value as the number of the iteractions rises.

The analysis of the noise influence on the quality of the image was performed by the CNR parameter on the three simulations proposed. The results are shown by the Fig. 9. By this Fig., it is possible to observe that even the data obtained by the simulation with no collimator and with the slit collimator reaches the same CNR value in the first iteractions, this values decreases rising the number of the iteractions, however the CNR of the simulation with no collimator decreases more than the slit collimator due to the growth of the noise. The CNR for the hole collimator reaches a higher CNR value, however as the number of iteractions rises, the noise decreases this value.

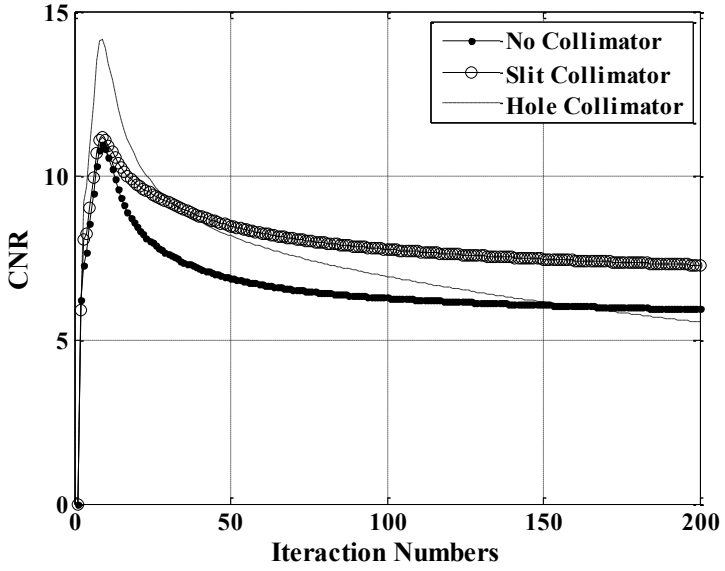

Figure 9: CNR analysis for (a) no collimator; (b) slit collimator and (c) hole collimator

The spatial resolution of the reconstructed images was measured by the MTF (*f*). The MTF curves by the frequency spectrum ($plmm^{-1}$) of the simulations proposed of the iteraction number of 200 are presented by the Fig. 10.

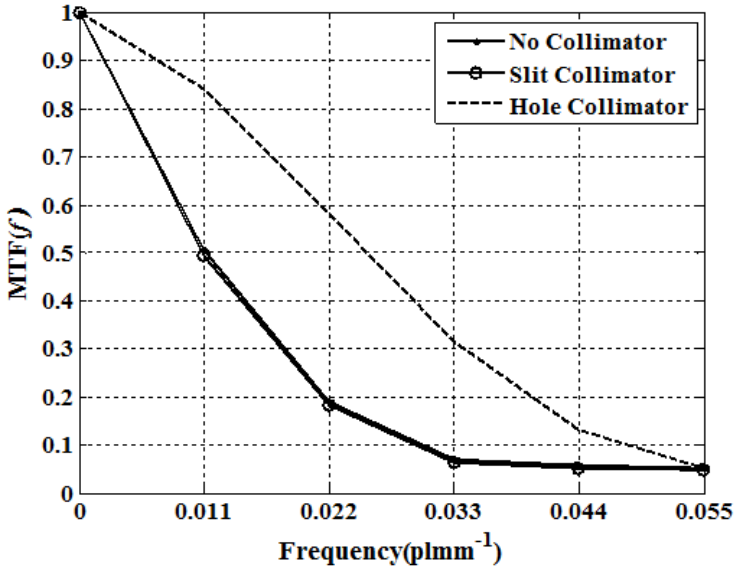

Figure 10: MTF analysis for (a) no collimator; (b) slit collimator and (c) hole collimator

By the Fig. 10, the data obtained by the hole collimator simulation presents a better spatial resolution in all frequency spectrum compared to the others simulations proposed, which presented the same MTF value for all the frequency range. The maximum spatial resolution of the system is measured at 10% of the MTF, in other words, the spatial resolution is calculated by the inverse of the frequency in 10% of the MTF. Thereby the resolution for the simulation of no collimator, slit collimator is about of 31.9mm and for the hole collimator is about 20 mm.

4. CONCLUSION

The results of the RMSE values showed that the data obtained with no collimator approaches to the theoretical values more compared to the other two simulations, which means that the experimental linear attenuation coefficient is close to the theoretical values.

The CNR analysis showed that for the data acquired with no collimator and with the slit collimator reaches the same CNR value, but the data with no collimator decreases more than the slit collimator as the number of iteraction rises, which means that no collimator suffer more noise growth than the data with the slit collimator. The data acquired with the hole collimator reaches a higher CNR value, however decreases mores than the other simulations, evidencing that the noise corrupt more the image with this kind of collimator compared to the others.

The spatial resolution of the instant non-scanning tomography system obtained with no collimator and with the slit collimator was the same for both, around 31.9mm, and for the hole collimator was around 20 mm, which means that this last simulation proposed presents a better spatial resolution.

ACKNOWLEDGMENTS

The authors express their acknowledgment to CNEN, FAPESP and IAEA for the financial support. The authors, Carlos Henrique de Mesquita and Margarida Mizue Hamada thank for their fellowship.

REFERENCES

1 KUMAR S.B., DUDUKOVIC M.P., Computer-assisted gamma and X-ray tomography: Application to multiphase flow. In Non-Invasive Monitoring of Multiphase Flows; Chaouki, J., Larachi, F., Dudukovic, M. P., Eds.; Elsevier: Amsterdam, The Netherlands, 1997; Chapter 2, p 48.

2 ISMAILA, GAMIOB J.C. Tomography for multi-phase flow measurement in the oil industry, Flow Meas. and Instr. 2002;16 145-155.

3 Velo A.F, Hamada M.M., Carvalho D.V.S., Martins J.F.T, Mesquita C.H., A portable tomography system with seventy detectors and five gamma-ray sources in fan beam geometry simulated by Monte Carlo method. Flow Meas. Instr. 53 (2017) 89-94.

4 JOHANSEN G.A., JACKSON P., (2004), Radioisotope Gauges for Industrial Process Measurements, John Wiley & Sons, 2004.

5 MAAD, R., JOHANSEN G.A. Experimental analysis of high-speed gamma-ray tomography performance. Meas. Sci. Technol, 2008; 19, 1-10.

6 FISCHER F, HOPPE D, SCHLEICHER E, MATTAUSCH G, FLASKE H, BARTEL R AND HAMPEL U. An ultra-fast electron beam x-ray tomography scanner. Meas. Sci. Technol, 2008. 19 1-11.

7 Disponível em <https://www.inl.gov/>. Acesso em 21 set 2017.

8 SALGADO, C.M., BRANDÃO L.E.B., SCHIRRU, R., PEREIRA, C.M.N.A.. CONTI C.C. Validation of a NaI(Tl) detector's model developed with MCNP-X code. Progress in Nuclear Energy, 2012. 59 19-25.

9 PELOWITZ, D.B. MCNP-X TM User's Manual, Version 2.5.0. 2005. LA-CP-05-0369. Los Alamos National Laboratory.

10 HADIZADEH YAZDI, M.H., MOWLAVI, A.A., THOMPSON, M.N., MIRI HAKIMABAD, H. Proper shielding for Na(Tl) detectors in combined neutron-gamma fields using MCNP. Nuclear Instruments and Methods in Physics, 2004. 522 447-454.

11 JEHOUANI, A., ICHAOUI, R., BOULKNEIR, M. Study of the NaI(Tl) efficiency by Monte-Carlo method. Applied Radiation and Isotopes, 2000. 53 (4-5), 887-891.

12 HADIZADEH YAZDI, M.H., MOWLAVI, A.A., THOMPSON, M.N., MIRI HAKIMABAD, H. Proper shielding for Na(Tl) detectors in combined neutron-gamma fields using MCNP. Nuclear Instruments and Methods in Physics, 2004. 522 447-454.

13 Smith, Steven W. The scientist and Engineer's Guide to Digital SignalProcessing. 1997

14 Christianson O., Chen J. J.S., Saiprasad G., Filliben J.J, Peskin A., Trimble C., Seigel E L., Samei E., An improved index of image quality for task-based performance of CT iterative reconstruction across three commercial implementations. 2015. 275 725-734

15 MAAD R., HJERTAKER B.T., JOHANSEN G.A. and OLSEN Ø. Dynamic characterization of a high speed gamma-ray tomography. Flow Measurement and Instrumentation, 2010. 21 538-545.

16 RICHARD S.L, HUSARIK D.B., YADAVA G., MURPHY S.N., and SAMEI E. Towards task-based assessment of CT performance: System and object MTF across different reconstruction algorithms. Med. Phys, 2012. 39 4115 - 4122.

17 SAMEI E., FLYNN M.J. and REIMANN D.A. A method for measuring the presampled MTF of digital radiographic systems using an edge test device. Med. Phys, 1998. 25(1), 102–113.